Journal of Supramolecular Structure 2:486–495 (1974)

STRUCTURAL STUDIES OF SPHERICAL VIRUSES

Stephen C. Harrison,* Anthony Jack,* Daniel Goodenough,† and Bartholomew M. Sefton‡

**Gibbs Laboratory, 12 Oxford St., Harvard University, Cambridge, Massachusetts 02138*

†Department of Anatomy, Harvard Medical School, Boston, Massachusetts 02115

‡Department of Biology, Massachusetts Institute of Technology, Cambridge, Massachusetts 02139

Structural studies of tomato bushy stunt virus and Sindbis virus are discussed in terms of the information they provide about specificity and control in virus and membrane assembly.

INTRODUCTION

Our ideas about macromolecular assembly rely on our knowledge of structure and spatial organization. This paper is a short progress report, to demonstrate how increasingly detailed structural information about spherical viruses directs our thinking about their assembly.

SIMPLE SPHERICAL VIRUSES: TBSV

Tomato bushy stunt virus (TBSV) is probably the most suitable of the simple viruses for atomic resolution structure analysis. It is built from 180 copies of a coat protein subunit (MW 41,000) and a single piece of RNA (MW 1.5×10^6) (1–3). There may also be a single copy of a large internal protein (MW 87,000) (4). The coat subunits form a T=3 icosahedral surface lattice. The symmetry of this lattice is represented by the polyhedron in Fig. 1. There are twofold, threefold, and fivefold axes of icosahedral symmetry as well as local ("quasi") twofold and threefold axes. The icosahedral threefold axes are actually *locally* sixfold. The subunit tips in TBSV are clustered near strict and local twofold positions, so that the surface shows prominent dimeric morphological units (Fig. 2). Electron microscopy (Fig. 3) and low-resolution x-ray diffraction (Fig. 4) have revealed an important aspect of the quasi-equivalent packing in TBSV: the outer pairs of subunits located near quasi-twofold positions lie 5 to 10 Å further from the center of the particle than those near strict twofolds (5,6). Indeed the rhombic triacontahedron, the polyhedron shown in Fig. 1, shows the surface lattice rather well. In TBSV, corresponding portions of subunits related by a local threefold axis lie approximately in a plane normal to the nearest strict twofold. The half-facet of the rhombic triacontahedron is therefore a good representation of the packing unit. A formula for

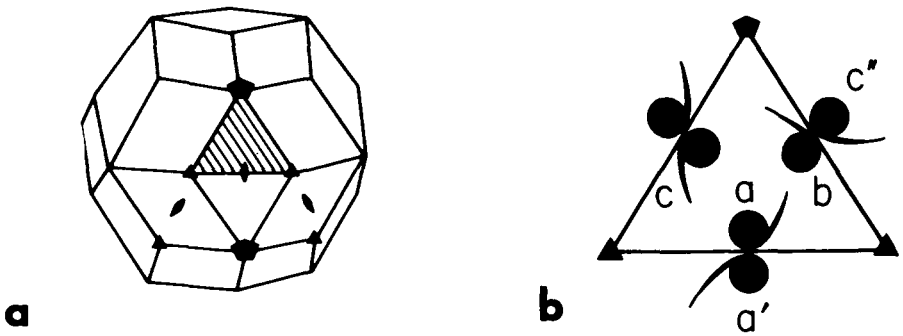

Fig. 1. (a) The rhombic triacontahedron with some of its symmetry elements shown. This polyhedron has icosahedral symmetry; the triangular half face represents a single fundamental domain, in the sense that the icosahedral symmetry elements will generate the entire figure from one such half-facet. (b) If we pack three subunits (a, b, c) into the half-facet in such a way that they are related by a threefold axis at its center, then a is related to a′ in one adjacent triangle by a strict twofold axis, and b is related to c″ by an essentially similar operation. The relation between b and c″ is only a local twofold axis, however; this may be seen by observing that it would interchange a fivefold and a threefold position if its domain extended beyond the immediately adjacent subunits.

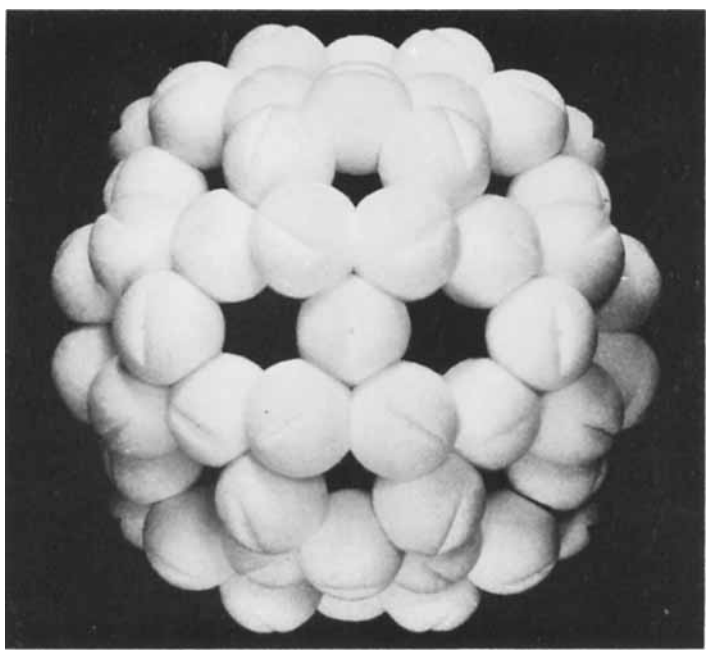

Fig. 2. Model indicating the dimer clustering of subunits on the surface of the TBSV particle. Each ball represents two subunits. Morphological units seen in the electron microscope correspond to these dimer clusters. Note that there are two sorts of balls in the model – those located on strict icosahedral twofold axes (thus representing two strictly equivalent subunit environments) and those located on local twofold axes (representing two quasi-equivalent environments). The balls have bonding surfaces to adjacent balls so directed that there is sharper curvature at the local diads than at the strict diads. If all the balls had the sharper curvature, they would form a sphere of smaller radius, with 30 balls (60 subunits) in a simple T=1 icosahedral surface lattice.

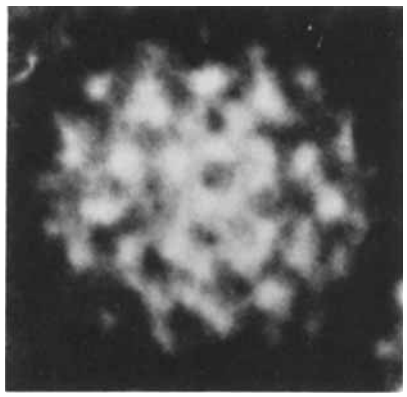

Fig. 3. Electron micrograph of TBSV particle, negatively stained with uranyl acetate. The view is down a twofold axis, exactly as in Fig. 2. Note the fivefold positions, where a trim surrounds a stain-filled cavity. In many images, stain has not penetrated this cavity.

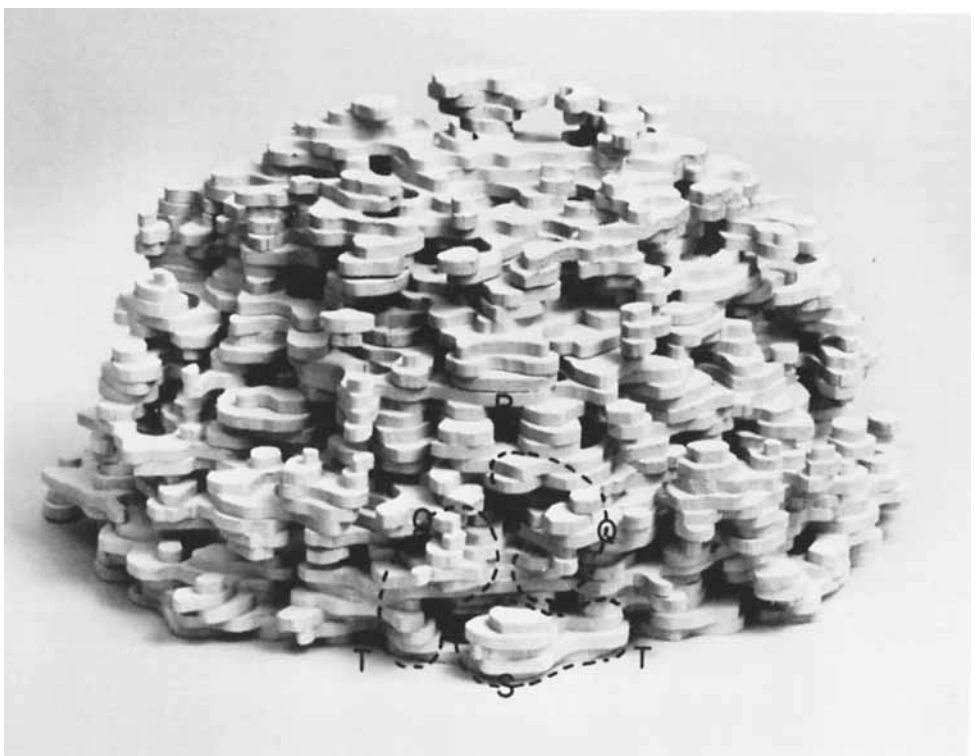

Fig. 4. Model of one-fourth of the TBSV particle, based on a 16 Å electron density map. The view is near a fivefold axis, i.e., slightly raised from the views in Figs. 2 and 3. The projecting subunit tips are indicated by S (near a strict twofold) and Q (near a local twofold). Compare the rim around the fivefold axis (P) with the electron micrograph in Fig. 3. This view of the model shows primarily the surface features, but the electron density map reveals the internal structure as well. Internal features of particularly high density show positions occupied by RNA. At this resolution we cannot identify unambiguous subunit boundaries, but possible outlines of three subunits are shown. The units penetrate, of course, well into the particle.

generating the structure would be: fill this triangle with three protein molecules, related to each other by a threefold axis normal to the triangle at its center; generate 59 other such triangles by the operations of icosahedral symmetry; compensate by appropriate bonding distortions for the very different curvature at the strict and local twofold positions, thus creating the differences among the three quasi-equivalent molecules. Of course, this formula does not imply that the actual pathway of assembly involves dimer or trimer intermediates.

We have recently computed a 16 Å electron density map of TBSV, using the multiple isomorphous replacement method aided by our knowledge of the high degree of noncrystallographic symmetry present in our crystals.* A view of a model, based on this map, appears in Fig. 4. We expect to refine further the 16 Å phases, and the description that follows may be subject to some revision. The protein subunits, dimer-clustered at the surface, project from the bulk of the particle. The outer tips (at r = 160–165 Å) bend away from each other, toward the local threefold. Lateral projections of the subunits extend from near the diads toward the five and quasi-sixfolds, forming the rim of a cavity that opens to the surface at these positions. At this resolution we cannot define the subunit boundary uniquely, but it is clear that tight dimer association does not extend along the full length of the subunits. There are cavities on both strict and quasi-twofold axes in the region of r = 135 Å, and the inner tips of the subunits (r = 90–100 Å) appear to spread toward the five and quasi-sixfold axes. Hexamer-pentamer clustering may therefore be important at inner radii.

The bonding of RNA to protein probably involves basic amino acid residues, of which sufficient are present in TBSV protein to neutralize most of the phosphate groups (7). By analogy with tobacco mosaic virus (TMV) we imagine that a series of specific phosphate binding sites lines grooves in the subunit surface. The location of these will be indicated by the distribution of RNA in the structure, which we can infer from high-density features in the map. The nucleic acid is not simply confined to an inner cavity. A cagelike network of density at about r = 110 Å and outward projections from this network at quasi-threefold positions suggest that much of the RNA is present in close association with protein subunits. The most important RNA binding sites may therefore be in the lateral surface of the subunits, where they face the quasi-threefolds. If this interpretation is correct, each subunit would have a groove for RNA on this surface, looping out from r ~ 110 Å to r ~ 135 Å and back. Depending on the details of the RNA conformation, these grooves might accommodate 10 to 15 nucleotides per subunit, and altogether 180 such sites would include about half of the RNA chain. The remainder of the nucleic acid chain loops into the center of the virus particle, where we know from small-angle x-ray scattering that it probably is present as a hydrated coil (8).

We have currently rather little information from physicochemical studies of TBSV assembly. One interesting piece of evidence comes from a polymorphic form of the protein in the closely related turnip crinkle virus (TCV). TCV, which has a structure essentially identical with TBSV, can be dissociated, and a small RNA-free particle obtained by reassociation of the subunits (9). These small particles contain 60 subunits of TCV protein, packed with dimer clustering in a T = 1 lattice. All subunits in such a lattice are of course strictly equivalent to each other, but the local bonding in the small particles is essentially the same as the quasi-equivalent bonding in TCV itself (5). The radius of these

*The fivefold axis in the icosahedral point group cannot be a symmetry element of the crystal. The crystallographic asymmetric unit in TBSV contains five icosahedral asymmetric units.

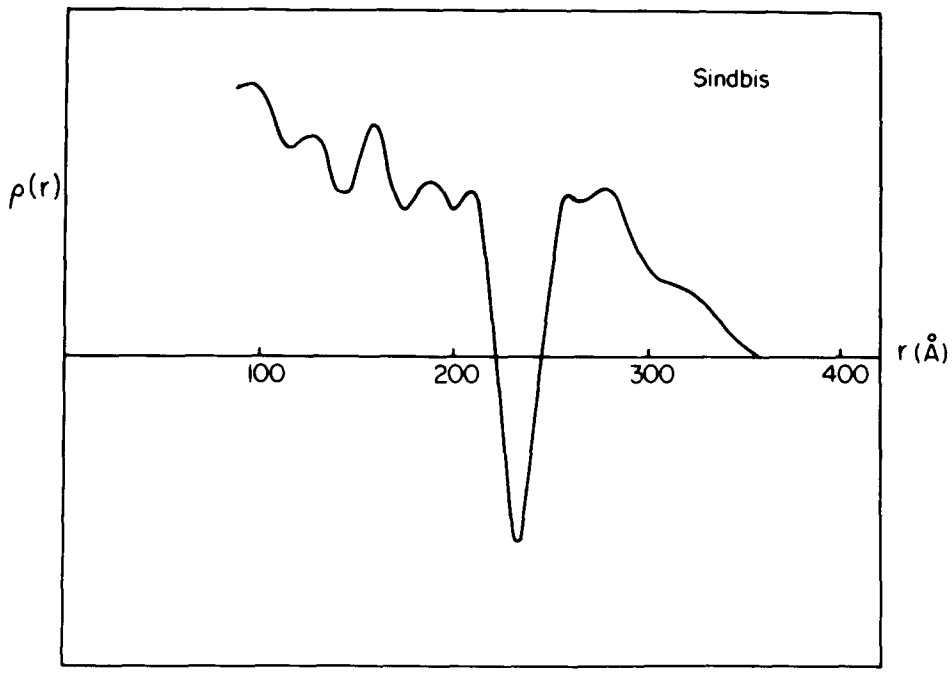

Fig. 5. The spherically averaged distribution of density in Sindbis virus, determined by x-ray scattering from a concentrated solution. Ordinate: electron density (arbitrary scale, with the density of water as the baseline); abscissa: radius (in Angstrom units). The deep minimum shows the position of a lipid bilayer.

small spheres is similar to the local radius of curvature at quasi-twofold positions in the virus. The bonding relation in small particles and at local diads in the whole virus (Q in Fig. 4) may therefore be a more stable configuration than the "flat" dimer bonding at strict diads in the virus (S in Fig. 4). The RNA–protein interactions could provide the free energy necessary to distort the protein–protein bonds. It might produce such a distortion if, for example, incorporation of RNA into the grooves facing a threefold axis were incompatible with the sharper curvature of the small particle. This sort of mechanism could account for the absence of a "top component" (empty T=3 shells) in TCV and TBSV, distinguishing them from, e.g., turnip yellow mosaic virus (TYMV) (10). We have no direct evidence for such speculation, but it does seem likely that, as with TMV (22), the protein configuration stable in the absence of RNA will be slightly different from the configuration in the virus itself. Such differences can be the elements of control mechanisms in assembly.

LIPID-CONTAINING VIRUSES: SINDBIS

Like many of the lipid-containing animal viruses, Sindbis matures by budding out through the plasma membrane of an infected cell (for a general review of viral budding, see Ref. 11). A nucleoprotein core preassembles in the cytoplasm from subunits of a single protein species (MW 30,000) and viral RNA (12). Electron micrographs of infected cells in thin section show these spherical cores both free in the cytoplasm and apposed to the inner surface of the cell membrane (13). During budding, the cores in effect wrap

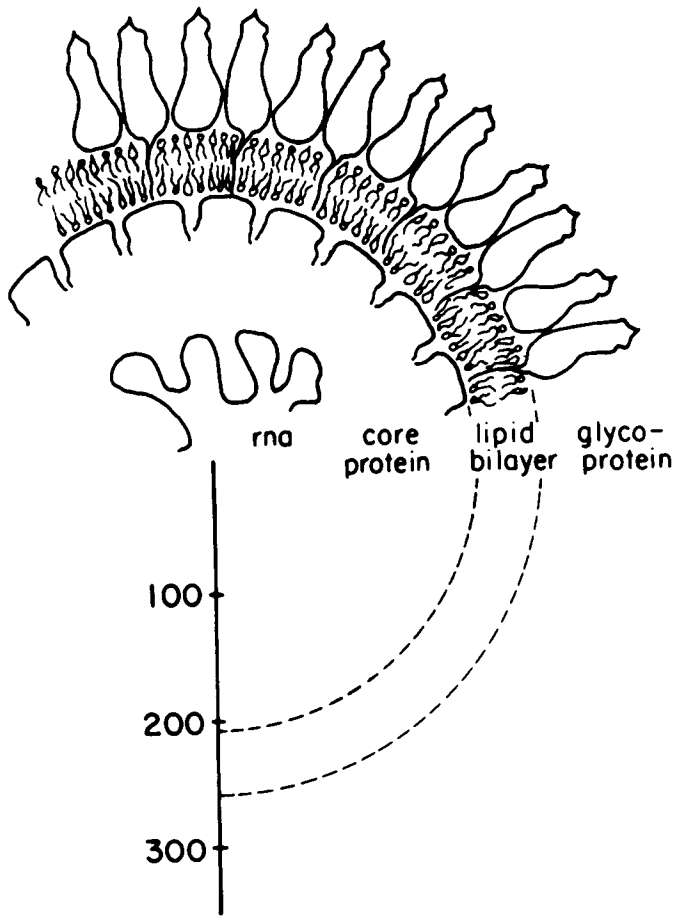

Fig. 6. A schematic representation of the radial organization in a Sindbis virus particle. The glycoprotein subunits have been represented as two sorts, one of which casts a hydrophobic "tail" across the bilayer. *This feature is purely symbolic:* we have no definite evidence for such a structure, and no evidence whether it might occur as part of one or both glycoprotein species. For a discussion of this possible structure, see text. Cf. also: Utermann, G. and Simons, K. J. Mol. Biol. 85:569 (1974).

themselves in a lipid bilayer coated on their outer surface with viral glycoprotein. In Sindbis there are two distinct glycoprotein species, both with a molecular weight of about 50,000 (14). No host proteins appear in the mature virus particle, but its lipids represent a random sample of the cellular plasma membrane (15,16).

The Sindbis particle is sufficiently regular in structure and spherical in shape that small angle x-ray scattering from solutions of the virus can be used to determine details of its radial organization (17). A plot of the spherically averaged density in the particle is shown in Fig. 5 and its interpretation, in terms of molecular arrangement, in Fig. 6. The lipids form a bilayer with polar group layers at $r \sim 210$ Å and $r \sim 258$ Å. The amount of lipid in the virus is just sufficient to form a complete spherical layer with these dimensions. We know from electron micrographs and from small angle x-ray measurements (Harrison and Sefton, unpublished) that the core is a relatively smooth-surfaced sphere with an outer radius of 200 ± 5 Å. Thus, the core interacts directly with the

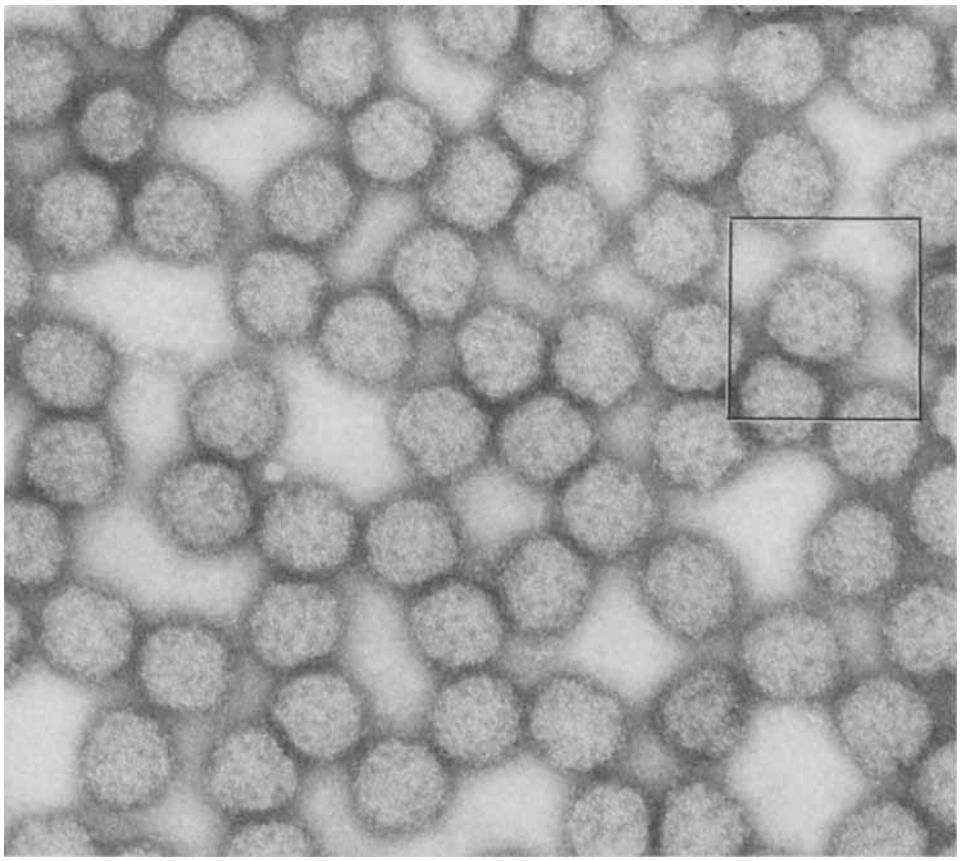

Fig. 7. Electron micrograph of a field of Sindbis particles, lightly fixed with glutaraldehyde (0.1%, dialysed away from dilute virus before concentrating by centrifugation) and negatively stained with uranyl acetate. 200,000 ×.

inner polar groups of the membrane lipid bilayer. The core protein therefore serves two functions: it encapsulates the RNA, like the coat of many small viruses, and it lines the inner membrane surface, like the M protein in influenza and vesicular stomatitis virus (11) or spectrin in the red blood cell.

What is the surface organization of Sindbis inner and outer proteins? Since the spherical cores self-assemble from subunits of a single protein species, we expect an icosahedral design. Our present electron micrographs of isolated cores are not quite good enough to reveal the surface lattice, but characteristic and reproducible images do indicate a regular structure. Accurate compositional data are available for the closely related Semliki Forest Virus (SFV). These indicate about 240 subunits per core, consistent with a T=4 surface lattice (18). Since x-ray scattering studies of SFV show a radial density distribution identical to Sindbis (Harrison and Kääriäinen, unpublished) and since the viruses are chemically as well as biologically similar, we suggest a T=4 structure for both nucleocapsids. We need not expect an icosahedral design for the outer glycoprotein, since its organization might be determined by interactions with the lipid bilayer, specific lateral interactions between glycoprotein subunits having a subsidiary role. Electron micrographs of Sindbis do indicate, however, a regular clustering, and the images can be interpreted by

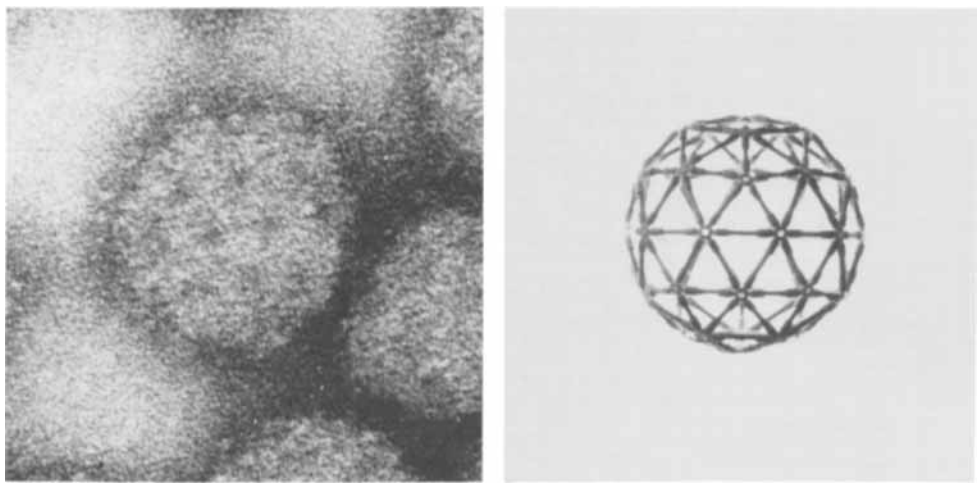

Fig. 8. One particularly common type of image from fields such as the one in Fig. 7, compared with a view of a skeletal model of a T=4 icosahedral surface lattice. Four sixfold positions superpose along the equator of this image, and three superpositions of fives and sixes will occur in rows above and below these four. The top and bottom of the image should be indistinct. A twofold view of a T=3 lattice will be at first sight similar, but the points above and below the center should be clearly identifiable as five-coordinated.

assuming that stain-penetrable pockets are present on the five- and local sixfold axes (Fig. 7). In such a structure, the most frequently found view superposing these positions on upper and lower surfaces of a particle will be the view along one of the two sorts of quasi-diads (Fig. 8). This is in fact the most common identifiable image in fields of Sindbis, such as the one shown in Fig. 7, where we can also see particles viewed along quasi-sixfold axes. Similar pictures of SFV have been obtained by von Bonsdorff (19). The core protein and each of the two glycoproteins are present in equimolar quantities in Sindbis virions. Inner and outer T=4 icosahedral surface lattices are therefore consistent with the chemical composition.

Do the internal and external proteins communicate accross the membrane? A number of observations indicate that protein can occupy only a relatively small fraction of the bilayer region. The position and total volume of the bilayer, shown by x-ray diffraction, can be compared with the lipid content of the virus particle: we estimate that no more than about 10% of the bilayer region may be occupied by nonlipid components. In other words, the center of the bilayer could accommodate a single loop of polypeptide chain from each glycoprotein subunit, but a much larger amount of buried protein would be inconsistent with the observed dimensions and densities (17). Freeze-fracture electron microscopy confirms this conclusion. Fractured membranes of infected cells show numerous intramembranous particles in the cleavage plane (21). Virus particles have smooth fracture faces (Fig. 9). Moreover, images of budding virus particles show intramembranous particles in regions adjacent to the buds but not in the emerging particles themselves (21). Since a pliant piece of polypeptide chain would not be contrasted by shadowing and replication, these results are consistent either with the presence of a narrow hydrophobic tail on the glycoprotein or with a continuous lipid bilayer, but they rule out extensive protein penetration. Some evidence for such a tail in SFV glycoprotein has been obtained by the Helsinki group (20). They have shown that a small leucine and isoleucine-rich polypeptide

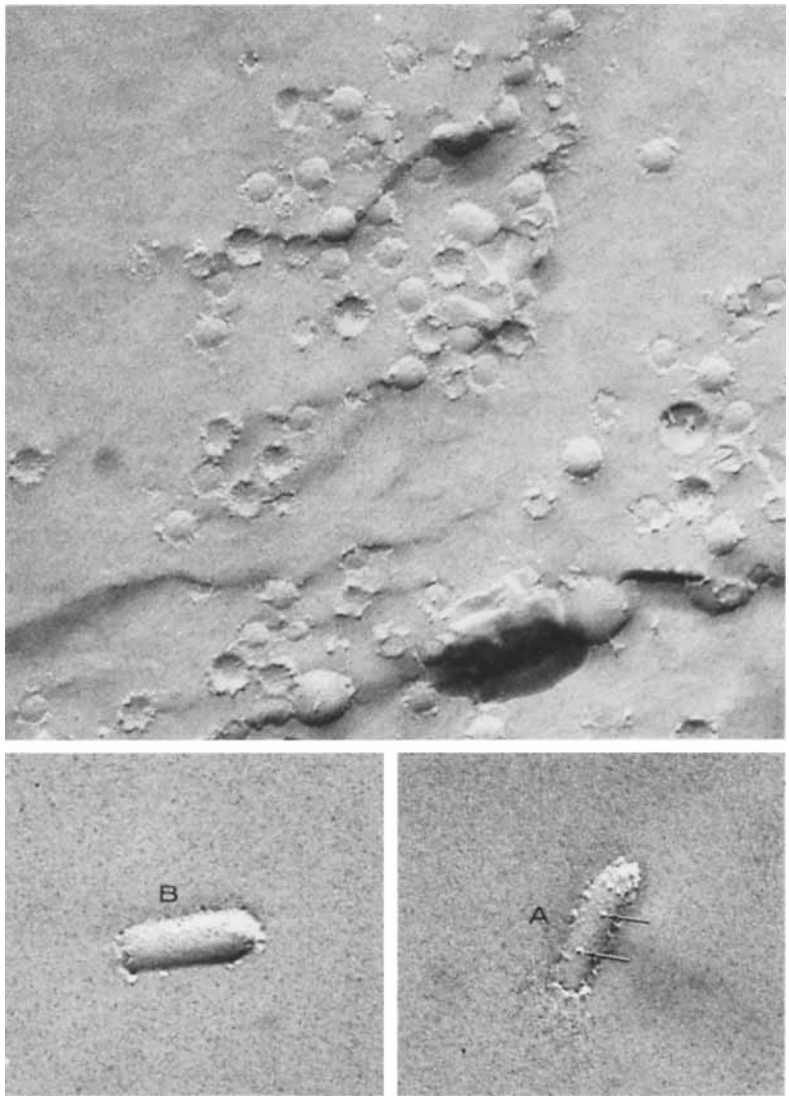

Fig. 9. Freeze-fracture electron micrographs of Sindbis (top, 81,000 ×) and, for comparison, two vesicular stomatatis virions (bottom, 135,000 ×), showing the A (convex) and B (concave) fracture faces. The fractured viral membranes are essentially free of intramembranous particles, although one or two such particles are sometimes seen on VSV. Note the "corona" of spikes at the edges of fractured Sindbis.

remains bound to virions after removal of the outer spikes with thermolysin. Such results do not show whether this polypeptide extends across the bilayer or resides only in the outer part of the membrane.

To explain specificity in budding, it is necessary to assume a local rearrangement of membrane, permitting the core to recognize those regions that contain only viral glycoprotein. We can imagine two possible mechanisms. The first invokes a direct contact between the core subunits and a glycoprotein tail. If the inner and outer surface lattices are indeed

similar, the structure will permit regular interactions between each core subunit and each pair of glycoproteins. The second invokes a recognition of membrane patches that have been modified by exclusion of host cell protein. If the host proteins interact across the membrane, then incompatibility of one viral protein with host structures will create a region of increased affinity for the others.

The interactions that determine recognition of inside and outside structures may also be sufficient to complete the rounding-off of the Sindbis virus particle. The core itself is a spherical structure, and provided that its interaction with the membrane is a reasonably strong one, it is unnecessary to invoke participation of other membrane components (e.g., microfilaments, etc.); that is, we can describe the final stages of budding as a straightforward self-assembly process. The core wraps itself in a membrane by virtue of specific interactions with a viral-glycoprotein-substituted bilayer. These interactions involve contacts with inner lipid polar groups and with a glycoprotein tail, if present. The free energy of such contacts could drive the extrusion of the Sindbis virus particle.

ACKNOWLEDGMENTS

We are grateful to C. Shutt for discussions and to H. Bailey for construction of the TBSV model. This work was supported in part by Public Health Service Grant CA-13202 (to S. C. Harrison) and in part by Grant No. GB34273 from the NSF Program in Human Cell Biology. S. C. Harrison acknowledges a PHS Research Career Development Award (CA-70169). A. Jack is a Jane Coffin Childs Postdoctoral Research Fellow, and B. M. Sefton is a Damon Runyon Postdoctoral Fellow.

REFERENCES

1. Weber, K., Rosenbusch, J., and Harrison, S. C., Virology 41:763 (1970).
2. Butler, P. J. G., J. Mol. Biol. 52:589 (1970).
3. Dorne, B., and Pinck, L., FEBS Lett. 12:241 (1971).
4. Ziegler, A., Harrison, S. C., and Leberman, R., Virology, (in press).
5. Crowther, R. A., and Amos, L., Cold Spring Harbor Symp. Quant. Biol. 36:489 (1971).
6. Harrison, S. C., Ph.D. Thesis, Harvard University (1967).
7. Michelin-Lausarot, P., Ambrosino, C., Steere, R. L., and Reichmann, M. E., Virology 41:160 (1970).
8. Harrison, S. C., Cold Spring Harbor Symp. Quant. Biol. 36:495 (1971).
9. Leberman, R., Symp. Soc. Gen. Microbiol. 18:183 (1968).
10. Kaper, J., Proc. 8th FEBS Meeting, Amsterdam 27:19 (1972).
11. Lenard, J. and Compans, R. W. Biochem. Biophys. Acta (in press).
12. Strauss, J. H., Burge, B. W., Pfefferkorn, E. R., and Darnell, J. E., Proc. Nat. Acad. Sci. 59:533 (1968).
13. Acheson, N. H., and Tamm, I., Virology 32:128 (1967).
14. Schlesinger, M. J., Schlesinger, S., and Burge, B., Virology 47:539 (1972).
15. Pfefferkorn, E. R., and Clifford, R. L., Virology 23:217 (1964).
16. Quigley, J. P., Rifkin, D. P., and Reich, E., Virology 46:106 (1971).
17. Harrison, S. C., David, A., Jumblatt, J., and Darnell, J. E., J. Mol. Biol. 60:523 (1971).
18. Laine, R., Söderlund, H., and Renkonen, O., Intervirology 1:110 (1973).
19. von Bonsdorff, C. H., Commentationes Biologicae Societatis Scientiarum Fennicae 74:1 (1973).
20. Gahmberg, C. G., Utermann, G., and Simons, K., FEBS Lett. 28:179 (1972).
21. Brown, D. T., Waite, M. R. F., and Pfefferkorn, E. R., J. Virol. 10:524 (1972).
22. Klug, A., and Durham, A. C. H., Cold Spring Harbor Symp. Quant. Biol. 36:449 (1971).